Cell Motility and the Cytoskeleton 66: 48–61 (2009)

Polarized MT1-MMP-CD44 Interaction and CD44 Cleavage During Cell Retraction Reveal an Essential Role for MT1-MMP in CD44-Mediated Invasion

Raquel Marrero-Diaz,[1] Jose J. Bravo-Cordero,[1] Diego Megías,[1] Maria A. García,[1] Ruben A. Bartolomé,[2] Joaquin Teixido,[2] and María C. Montoya[1]*

[1]*Confocal Microscopy and Cytometry Unit, Biotechnology Programme, Centro Nacional de Investigaciones Oncológicas (CNIO), Madrid, Spain*
[2]*Department of Cellular and Molecular Physiopathology, Centro de Investigaciones Biológicas, Consejo Superior de Investigaciones Científicas, Madrid, Spain*

The adhesion molecule CD44 and the membrane-type matrix metalloproteinase MT1-MMP act coordinately in tumor cells to promote cell invasion through a yet unclear mechanism. We are interested in studying the interplay between CD44 and MT1-MMP in carcinoma cells embedded in HA containing three-dimensional collagen I matrices (3D HA-Col I) by time-lapse confocal microscopy imaging. Here we report the in vivo interaction between CD44 and MT1-MMP, revealed by fluorescence resonance energy transfer (FRET) microscopy. MT1-MMP interacts with CD44 preferentially at the trailing edge of the invading tumor cells during rear retraction and on membrane fragments released during the invasion process. A fluorescent biosensor designed to monitor the proteolytic processing of CD44 by live cell imaging demonstrates that cleavage of the CD44 extracellular domain is enriched in the retracting rear ends of invasive tumor cells. Invasion assays showed that MT1-MMP mediates CD44-dependent tumor-cell invasion, whereas CD44 is not essential for MT1-MMP-mediated invasion of 3D HA-Col I matrices. Together, our results support a role for MT1-MMP in cell retraction during CD44-mediated cell invasion. Cell Motil. Cytoskeleton 66: 48–61, 2009.

Key words: matrix metalloproteinases; MT1-MMP; migration; CD44; tumour; invasion

INTRODUCTION

Migration is a process with complex spatial and temporal regulation and it plays a prominent role in the pathophysiology of tumor cell invasion and metastasis. Cell invasion relies on a highly polarized cell morphology and involves a series of important events, including (i) cell adhesion to the extracellular matrix (ECM) and actin polymerization, leading to membrane protrusion of the leading edge; (ii) degradation of extracellular components by metalloproteinases at the leading edge to release matrix steric resistance, allowing the advancing front of the cell to move forward [Wolf et al., 2007]; and (iii) detachment of the trailing edge, which involves mecha-

Additional Supporting Information may be found in the online version of this article.

Contract grant sponsor: Fondo de Investigaciones Sanitarias (FIS), Contract grant numbers: PI061839; Contract grant sponsors: Ministry of Science and Technology of Spain (MCYT), Fundación Canaria Dr. Manuel Morales.

*Correspondence to: Maria C. Montoya, Confocal Microscopy and Cytometry Unit, Biotechnology Programme, Spanish Nacional Cancer Research Center (CNIO), C/ Melchor Fernández Almagro 3. Madrid E-28029, Spain. E-mail: mmontoya@cnio.es

Received 29 May 2008; Revised 3 October 2008; Accepted 15 October 2008

Published online 20 November 2008 in Wiley InterScience (www.interscience.wiley.com).
DOI: 10.1002/cm.20325

nisms such as the disassembly of adhesion structures and the proteolytic cleavage and internalization of adhesion receptors [Friedl and Wolf, 2003]. Proteolytic cleavage is a key mechanism underlying the functional regulation of a number of membrane adhesion receptors. Shedding is particularly active in invasive cancer cells, where cell-surface components, including CD44 and MT1-MMP, are continually released into the extracellular medium [Friedl et al., 1997; Taraboletti et al., 2002; Nagano and Saya, 2004; Bravo-Cordero et al., 2007]. CD44 is a cell adhesion molecule for hyaluronan (HA), collagen, laminin, and fibronectin, and plays an important role in the migratory, invasive, and metastatic behavior of cancer cells [Marhaba and Zoller, 2004]. CD44 binds to the ezrin/radixin/moesin (ERM) proteins [Tsukita et al., 1994; Legg et al., 2002], which act as linkers to the actin cytoskeleton and to membrane type I matrix metalloproteinase (MT1-MMP), which proteolytically cleaves its extracellular domain stimulating cell motility [Kajita et al., 2001].

MT1-MMP is a critical factor in the invasion machinery of tumor cells and is involved in both matrix degradation and the processing of cell-surface receptors. Given its potential degradative activity, MT1-MMP expression at the cell surface is tightly regulated by intracellular vesicle trafficking [Itoh and Seiki, 2006]. MT1-MMP localization to the invasive front allows localized proteolysis of the extracellular matrix, which is a key to its invasion-promoting activity [Nakahara et al., 1997; Lehti et al., 2000; Mori et al., 2002]. Previous studies have showed that the delivery of MT1-MMP to the invasive front is regulated through its association with CD44 [Kajita et al., 2001; Mori et al., 2002; Suenaga et al., 2005]. CD44 would provide a link of MT1-MMP to the actin cytoskeleton through its interaction with ERMs thereby acting as a platform on which MT1-MMP produces matrix degradation [Itoh and Seiki, 2006]. We uncovered an alternative pathway that accounts for the recruitment of MT1-MMP to invasive structures in 3D Col I invading tumor cells, namely the Rab8-mediated intracellular exocytic traffic [Bravo-Cordero et al., 2007]. Although the localization of MT1-MMP to the leading edge has been extensively studied, its role in other membrane localizations has not been addressed.

Here, we investigate the in vivo interaction between CD44 and MT1-MMP using fluorescence resonance energy transfer (FRET) technology. A novel reporter was designed for imaging the proteolytic processing of CD44 by live cell microscopy. We show that the MT1-MMP interaction with CD44 and the MT1-MMP-mediated proteolytic processing of CD44 occurs preferentially at the retracting cell rear and that MT1-MMP is essential for CD44-mediated cell invasion.

MATERIALS AND METHODS

Cell Culture, Transfection, RNA Interference, and Collagen Inclusion

Breast adenocarcinoma MDA-MB-231 cells, human fibrosarcoma HT-1080 cells, and human melanoma BLM cells were maintained in Dulbecco's modified Eagle's medium (DMEM) supplemented with 10% fetal bovine serum (FBS) and 1% Penicillin/Streptomycin. The cells were transfected using Lipofectamine 2000 (Invitrogen, Carlsbad, CA) according to manufacturer's instructions. Twenty-four hours after transfection, the cells were trypsinized and mixed with newly prepared HA-Col I solution (2.4 mg/mL bovine Col I [Vitrogen, Palo Alto, CA], 1 mg/mL HA [Sigma-Aldrich, St Louis, MO], 1 × RPMI, 19 mM Hepes [Gibco, Invitrogen, Carlsbad, CA], 0.19% sodium bicarbonate [Sigma-Aldrich], 5% FBS), which was then allowed to polymerize for 2 h at 37°C (3D HA-Col I), plated onto prepolymerized 3D HA-Col I, or onto uncoated coverslips.

Small interfering RNA (siRNA) duplexes to human MT1-MMP and a control siRNA were designed [Bartolome et al., 2006], and purchased from Ambion (Austin, TX). MDA-MB-231 cells were transfected with siRNAs (20 μM) using X-tremeGene siRNA transfection reagent (Roche Diagnostics, Panzberg, Germany) according to the manufacturer's instructions. After 24 h, cells were transfected with Orange-CD44-GFP construct. 48 h after transfection of siRNAs, cells were either embeded in 3D HA-Col I and analyzed using confocal microscopy imaging to quantitate CD44 shedding or lysed and subjected to western blot analysis for biochemical studies.

Reagents and Antibodies

The reagents used included phorbol myristate acetate (PMA), ionomycin (IO) (Sigma-Aldrich), and GM6001, an MMP inhibitor (Chemicon, Millipore, Billerica, MA). Antibodies used included mouse anti-human CD44 antibody (HP2/9) and rabbit anti-human-ERM antibody (90/3), kindly provided by Dr. F. Sánchez Madrid, Hospital de la Princesa, and Lem-2/15 mouse anti-MT1-MMP antibody [Galvez et al., 2002]. Rabbit anti-caveolin-1 antibody was provided by Dr. M.A. del Pozo, Centro Nacional de Investigaciones Cardiovasculares. Rabbit anti-GFP antibody (Abcam, Cambridge, UK) and mouse anti-tubulin DM1a were from Sigma-Aldrich.

Cloning DNA Constructs

The cDNA of the standard form CD44 was PCR amplified from the CD44 pRc/CMV vector provided by Dr. T Mizoi, using the oligonucleotide primers (forward) 5′-GGAGCTCATGGACAAGTTTTGGTG-3′ and (reverse) 5′- ATGAAGATTGGGGTGTTGGTACCG-3′,

and was cloned into the ECFP-N1 and EGFP-N1 vectors (Clontech, Takara Bio, Otsu, Shiga, Japan) at the *Kpn*I/*Sac*I restriction sites. The CD44-mRFP construct was obtained by subcloning mRFP into the EGFP-N1 restriction sites to generate CD44-GFP. The CD44 shedding reporter was generated by amplifying the cDNA of mOrange fluorescent protein using the oligonucleotide primers (forward) 5′-CCATCGATATGGTGAGCAAGGG CGAG-3′ and (reverse) 5′-CCATCGATCTTGTACAG CTCGTCCATG-3′, from the pRSET-B-mOrange vector (Invitrogen), and inserted into the CD44 pRc/CMV vector at the *Cla*I restriction site to generate mOrange-CD44. mOrange-CD44 cDNA was amplified and inserted into the EGFP-N1 vector at the *Kpn*I/*Sac*I restriction sites, generating Orange-CD44-GFP. Tandem GFP-Orange was generated by amplifying the cDNA of mOrange fluorescent protein using the oligonucleotide primers (forward) 5′-GGGGTACCATGGTGAGCAA GGGC-3′ and (reverse) 5′- CGGGATCCTTACTTGTA CAGCTCGTC-3′ and was then inserted into the EGFP-N1 vector at the *Kpn*I/*Bam*HI restriction sites. The MT1-MMP-YFP, CFP, GFP, and mRFP constructs have been described elsewhere [Bravo-Cordero et al., 2007]. Full-length moesin-GFP, Cav-1-mRFP, and VSV-G-YFP were kindly provided by Dr. F. Sánchez Madrid, Dr. M.A. del Pozo, and Dr. R. Pepperkok, respectively. All constructs were verified by DNA sequencing.

Immunofluorescence and Microscopy

For fixed-cell FRET analysis, MDA-MB-231 cells expressing CD44-GFP and MT1-MMP-mRFP were plated on prepolymerized 3D HA-Col I, fixed, and stained with either mouse anti-human-CD44 antibody (HP2/9) and anti-MT1-MMP antibody (Lem-2/15) previously conjugated with Alexa 488 and Cy3 using protein monoclonal antibody labeling kits from Invitrogen and Jackson ImmunoResearch (Amersham Biosciences, Uppsala, Sweden), respectively. Control cells expressing CD44-mRFP/moesin-GFP and CD44-GFP/Cav-1-mRFP were stained with rabbit anti-ERM (90/3), mouse anti-CD44 (HP2/9), and rabbit anti-caveolin-1 antibodies, and visualized with secondary antibodies labeled with Alexa 488 and Cy3. MDA-MB-231 cells expressing Orange-CD44-GFP were plated on coverslips, fixed, and stained with mouse anti-human-CD44 antibody (HP2/9) and visualized with secondary antibody labeled with Alexa 633. Images were collected with Leica SP2 and SP5 spectral confocal microscopes using 63× objective lenses (Leica, Mannheim, Germany).

λFRET Microscopy and Image Analysis

λFRET analysis was performed as previously described [Megías et al., in press]. In brief, λFRET measurements were based on spectral imaging of a sample containing both donor (Alexa 488-CFP-GFP) and acceptor (Cy3-YFP-mRFP) species, which were excited using λD488/λA543 laser lines (for the pairs Alexa 488/Cy3 and GFP/mRFP) or λD458/λA514 laser lines (for the pair CFP/YFP). For each excitation wavelength, we obtained one reflection image and a λ series of fluorescence images by defining detection windows of 25 nm in width, ranging from 465 to 650 nm. Raw fluorescence images were first corrected for background. Fluorescence intensity was then plotted for each pixel in the spectral data set of the images against the median wavelength value for each emission window to form the raw fluorescence spectra. The raw FRET spectra were then processed to obtain pure spectra by applying leak-through and cross-excitation corrections. The FRET efficiency calculation based on pure spectra analysis generated a pixel-based calculation of FRET efficiency. IDL software (ITT Visual Information Solutions, Boulder, CO) was used to integrate the computerized image analysis functions into a single ''custom-made'' algorithm that could be applied to sets of images and a time-lapse image series to obtain FRET efficiency images.

Quantification of CD44 Shedding Using Confocal Microscopy Imaging

MDA-MB-231 cells expressing tandem GFP-Orange or Orange-CD44-GFP were preincubated or not with the MMP inhibitor GM6001 (10 μM) for 24 h, plated on coverslips, and treated with PMA (10 or 20 ng/mL) or ionomycin (50 nM) for 2 h at 37°C. The cells were plated on coverslips either uncoated or coated with HA or 3D HA-Col I in the presence or absence of Lem-2/15 anti-MT1-MMP antibody (10 μg/mL). To control for the differences in quantum yields of GFP and Orange fluorescence, we used cells expressing the tandem GFP-Orange construct to define image acquisition settings in which the intensities of GFP and Orange were equivalent. The quantitative evaluation of CD44 proteolytic processing was measured as the GFP/Orange ratio fluorescence intensities obtained from microscopic images of invasive cells expressing Orange-CD44-GFP, using the GFP-Orange construct in a ratio (1:1) as the control. GFP/Orange ratio images were obtained with MetaMorph Offline Premier software (Molecular Devices Corporation, Downingtown, PA). The ratio image was built using the *4 Ratios with 64 Intensities* option, which has four distinct hues, each with 64 intensities visible in its contrast/threshold slider. The ratio images were pseudo-colored, ranging from 0 to 2.5, from 0 to 4, or from 0 to 8, where red and blue represent high and low ratio values, respectively. Finally, we used a low-pass fil-

ter of 3 pixels (width) × 3 pixels (height) to obtain the resultant ratio images.

Western Blot Analysis

HT-1080 cells stably expressing Orange-CD44-GFP or MDA-MB-231 cells transiently transfected with MT1-MMP or control siRNA and Orange-CD44-GFP for 48 h were preincubated or not with the MMP inhibitor GM6001 (10 μM) for 24 h and treated or not with 20 ng/mL PMA, a CD44-cleavage-stimulating agent, for an additional 2 h at 37°C. Cell lysates were isolated with lysis buffer (50 mM Tris [pH 7.4], 150 mM NaCl, 1 mM EDTA, 1% Triton, 2 mM $MgCl_2$) supplemented with protease inhibitors. Protein concentrations were determined using the Bio-Rad DC Protein assay kit. Cell lysates were separated by SDS-PAGE and transferred to a nitrocellulose membrane under semi-dry conditions. The membrane was then blocked with 5% nonfat milk in PBS-Tween 0.2% and incubated with polyclonal anti-GFP antibody (1/1000; Abcam), and monoclonal anti-tubulin DM1a antibody (1/10,000; Sigma). Alexa-Fluor-680-conjugated secondary antibodies were used to visualize and quantify the proteins with the Odyssey Infrared Imaging System (Li-COR, Biosciences, Lincoln, NE).

Cell Invasion Assays

Invasion assays of MDA-MB-231 and BLM cells transfected with the different constructs were performed in HA-3D-Col-I-coated 8 μm pore transwell chambers (Corning, Costar, New York, NY). Twenty-four hours after transfection, the cells were seeded at 5×10^4 cells/well in serum-free medium in the presence of 10 μg/mL blocking antibodies: anti-CD44 (HP2/9), anti-MT1-MMP (Lem-2/15), control isotype IgG1 or MMP inhibitor GM6001 (10 μM). The cells were allowed to transmigrate to 10% FBS medium for 48 h and were imaged by confocal microscopy. Invasion was quantified by the image analysis of GFP- or GFP-Orange-expressing cells counted at the top and bottom of the chamber using Imaris software (Bitplane AG, Zurich, Switzerland). The bars represent the percentage of invasive cells relative to the total number of fluorescent cells.

Statistical Analysis

All numerical values reported represent means ± S.E. The statistical significance of differences between the experimental and control values was evaluated using Student's t test. $P < 0.05$ was taken as the limit of statistical significance ($^*P < 0.05$; $^{**}P < 0.01$; $^{***}/^{+++}P < 0.001$).

RESULTS

Polarized Interaction Between MT1-MMP and CD44 During Tumor Cell Invasion

CD44 and MT1-MMP function in a coordinated manner to promote cell invasion, although the precise mechanism behind this interplay is as yet unclear [Kajita et al., 2001; Mori et al., 2002; Vivinus-Nebot et al., 2004]. To study the regulation of CD44 and MT1-MMP during the invasion process, we first expressed cyan fluorescent protein tagged CD44 (CD44-CFP) and yellow fluorescent protein tagged MT1-MMP (MT1-MMP-YFP) in breast carcinoma MDA-MB-231 cells and embedded them in three-dimensional (3D) hyaluronan (HA)-collagen 1 (Col I) matrices. The cells typically acquired a bipolar morphology, displaying a front or leading edge (LE) that determines the direction of movement and a rear or trailing edge (TE) that eventually retracts. Monitoring the molecular dynamics by live cell confocal imaging showed clear colocalization of CD44 and MT1-MMP during cell exploratory contacts with the ECM. Most interestingly, these studies revealed enrichment of both CD44 and MT1-MMP at the trailing edge of the cell preceding and during the detachment of the rear of the cell during migration (Fig. 1 and Supporting Video 1). Colocalization analysis at different membrane localizations is shown (Supporting Fig. 1). Although standard biochemical approaches have previously demonstrated that MT1-MMP forms a complex with CD44 via its hemopexin domain [Mori et al., 2002], there is still no in vivo evidence of the CD44-MT1-MMP interaction. To address this issue, we performed FRET studies, which allowed us to demonstrate this in vivo molecular interaction and analyze its sub-cellular localization. First, fixed MDA-MB-231 cells expressing either CD44-GFP, and monomeric red fluorescent protein tagged MT1-MMP (MT1-MMP-mRFP), moesin-GFP and CD44-mRFP, or CD44-GFP and caveolin-1 (Cav-1)-mRFP were analyzed using two different FRET analysis methods, namely, λFRET and acceptor photobleaching. We used a recently developed λFRET method [Megías et al., In press], because it is highly sensitive and reproducible, and unlike acceptor photobleaching method, it is applicable to live cell studies. CD44-Cav-1 produced negative FRET results, whereas CD44-moesin produced positive FRET results in cells plated on coverslips coated with Col I and HA (Fig. 2a). Although homogeneous FRET efficiency values were recorded for the CD44-moesin interaction, the CD44-MT1-MMP pair displayed a heterogeneous distribution of FRET efficiency values across the cell surface. For quantitative purposes, the two poles of the cells were classified as leading or trailing edges. Front/rear polarity was established by the direction of cell movement in live cell experiments or by

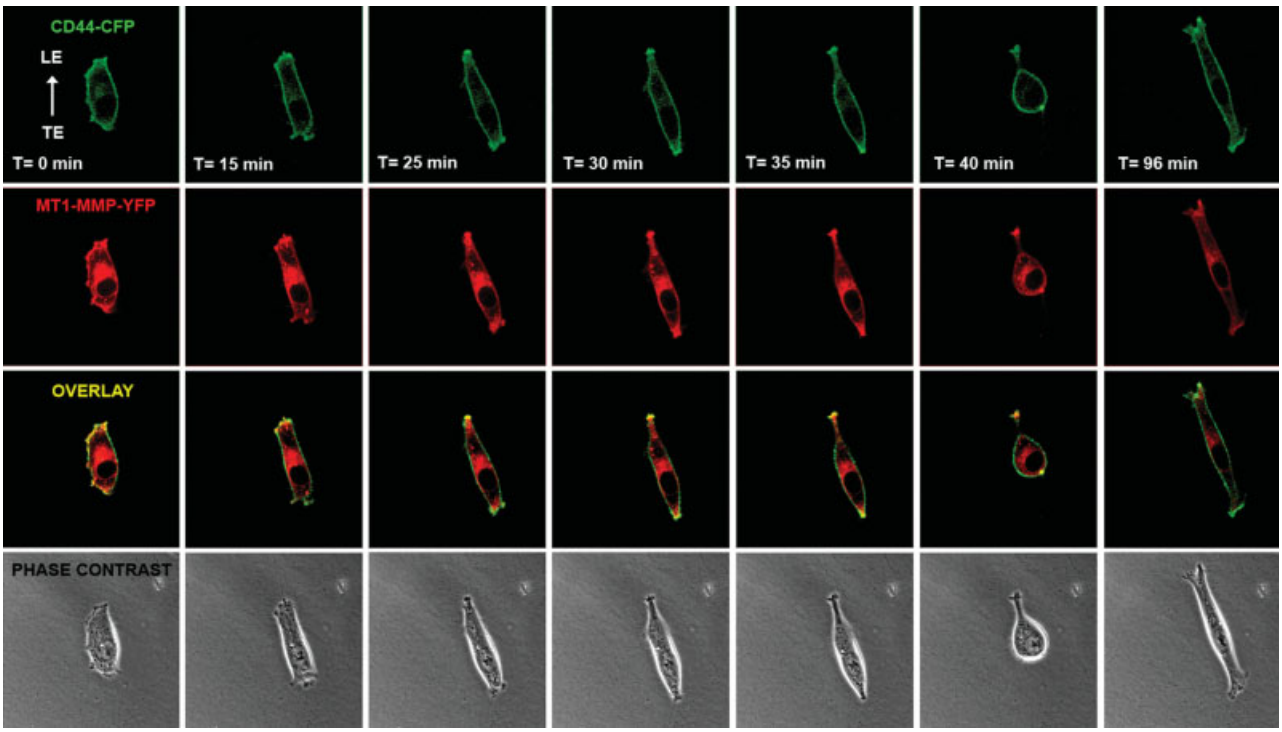

Fig. 1. Dynamics of CD44 and MT1-MMP localization in invading carcinoma cells. Breast carcinoma MDA-MB-231 cells were cotransfected with CD44-CFP and MT1-MMP-YFP, embedded in HA-3D Col I matrices, and analyzed by live cell confocal microscopy imaging. Representative CFP (green) and YFP (red) fluorescence images, their superimposition, and a transmitted light image showing collagen fibers (gray) obtained at the times indicated are shown. Position of the leading (LE) and trailing edges (TE) is indicated. The arrow indicates the direction of movement.

localizing the track of the membrane fragments deposited behind the migrating cell in fixed cell experiments. Membrane fragments that remain attached to the matrix after the retraction of the cell rear, in the process termed ripping (RIP), were also analyzed. CD44-MT1-MMP FRET efficiency values were significantly higher in the ripping and cell trailing edge compared with that in the leading front, where FRET analysis rendered low efficiency values (Fig. 2a). This interaction was also studied in human fibrosarcoma HT1080 cells. Exogenously expressed CD44-CFP and MT1-MMP-YFP, also displayed significant differences in FRET results measured at different membrane sub-domains (Fig. 2b).

To study the spatial and temporal regulation of this interaction, we performed FRET studies on live MDA-MB-231 cells expressing CD44-CFP and MT1-MMP-YFP. Consistent positive FRET efficiency values were recorded during the process of rear retraction in cells invading HA-3D Col I, confirming that the MT1-MMP-CD44 interaction takes place mainly at the trailing edges of migrating cells (Fig. 3a). As a control, we studied cells expressing CD44-mRFP and moesin-GFP. Although most CD44 and moesin accumulated at the cell poles, this was not traduced into higher FRET efficiency values in these areas, which remained constant during the migratory process regardless of their dynamic redistribution (Fig. 3b). These results together demonstrate that, ''in vivo,'' the CD44-MT1-MMP interaction is enriched at the rear of the cell and in the membrane fragments released into the extracellular medium by invasive cells.

MT1-MMP-Dependent Proteolytic Cleavage of the CD44 Extracellular Domain is Enriched at the Retracting Trailing Edges of Invading Tumor Cells

Because MMP inhibitors abolish CD44 processing and cell migration on HA, matrix metalloproteinase-dependent CD44 cleavage must play a critical role in tumor cell migration [Okamoto et al., 1999b; Kajita et al., 2001; Mori et al., 2002]. The polarized MT1-MMP-CD44 interaction reported here could be related to CD44 proteolytic processing at the cell rear. To directly address this issue, we generated a chimeric construct of CD44 tagged with both Orange and GFP fluorescent proteins at the N-terminal extracellular and C-terminal cytoplasmic domains, respectively (Figs. 4a and 4b). A GFP-Orange tandem was generated as a reference construct. GFP and Orange fluorescence images obtained with a

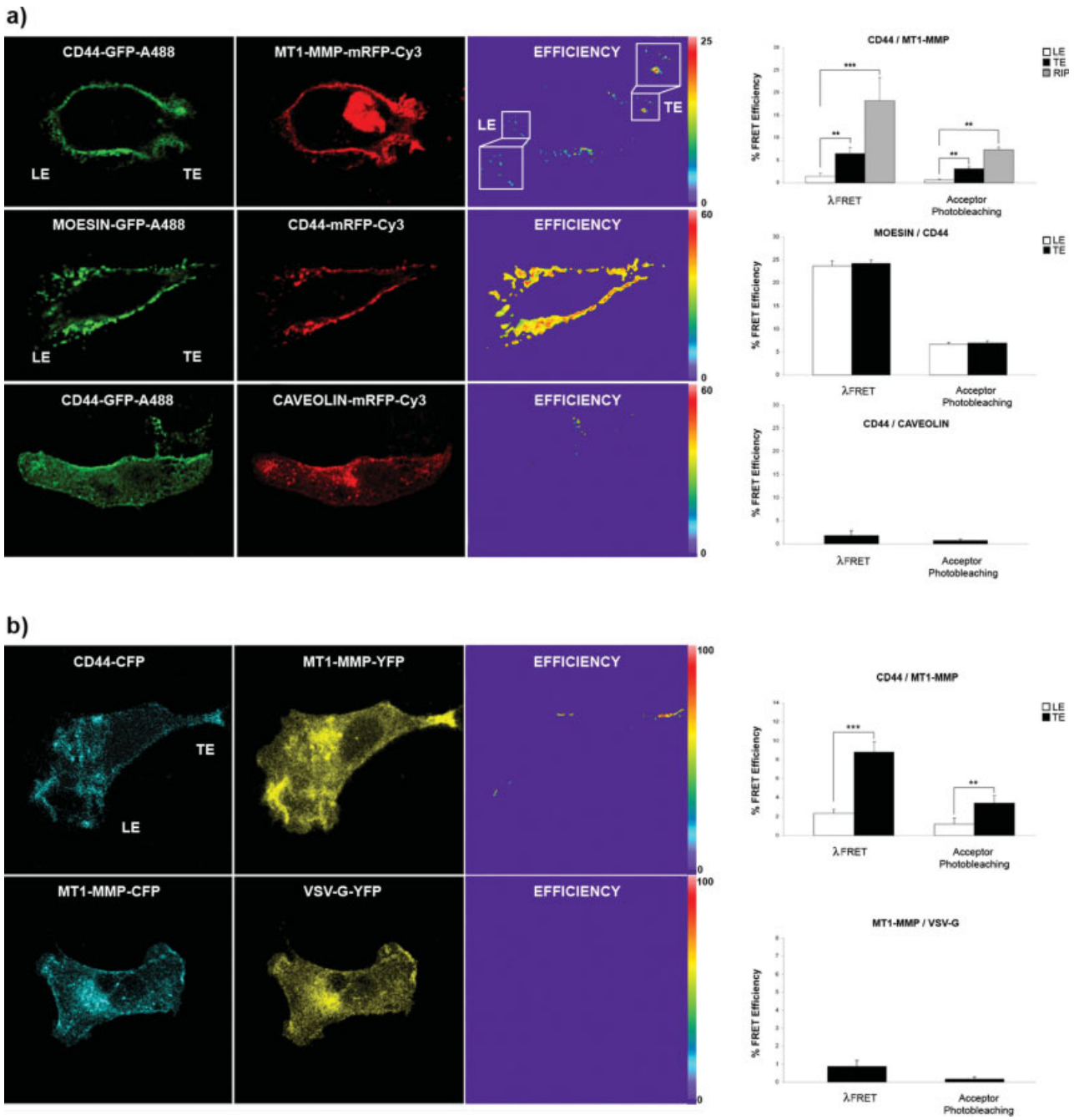

Fig. 2. Sub-cellular localization of the CD44-MT1-MMP interaction at the trailing edge of the cell. (**a**) Breast carcinoma MDA-MB-231 cells cotransfected with CD44-GFP and MT1-MMP-mRFP, moesin-GFP and CD44-mRFP, or CD44-GFP and Cav-1-mRFP, were plated on HA-Col-I-coated coverslips. The cells were fixed and stained with anti-CD44, anti-MT1-MMP, anti-moesin, or anti-caveolin antibodies labeled with Alexa 488 and Cy3. Representative donor (green) and acceptor (red) fluorescence and pseudo-colored FRET efficiency images are shown. Bar diagrams represent FRET values calculated at the leading and trailing edges (LE and TE, respectively) and ripping (RIP), using λFRET or acceptor photobleaching methods. (**b**) Human fibrosarcoma HT-1080 cells were transfected with either CD44-CFP and MT1-MMP-YFP or MT1-MMP-CFP and vesicular stomatitis virus G protein (VSV-G)-YFP. Representative CFP (cyan) and YFP (yellow) fluorescence and λFRET efficiency pseudo-colored images are shown. Bar diagrams represent the FRET efficiency values calculated using the λFRET or acceptor photobleaching methods at the indicated subcellular locations from 12 cells in three independent experiments.

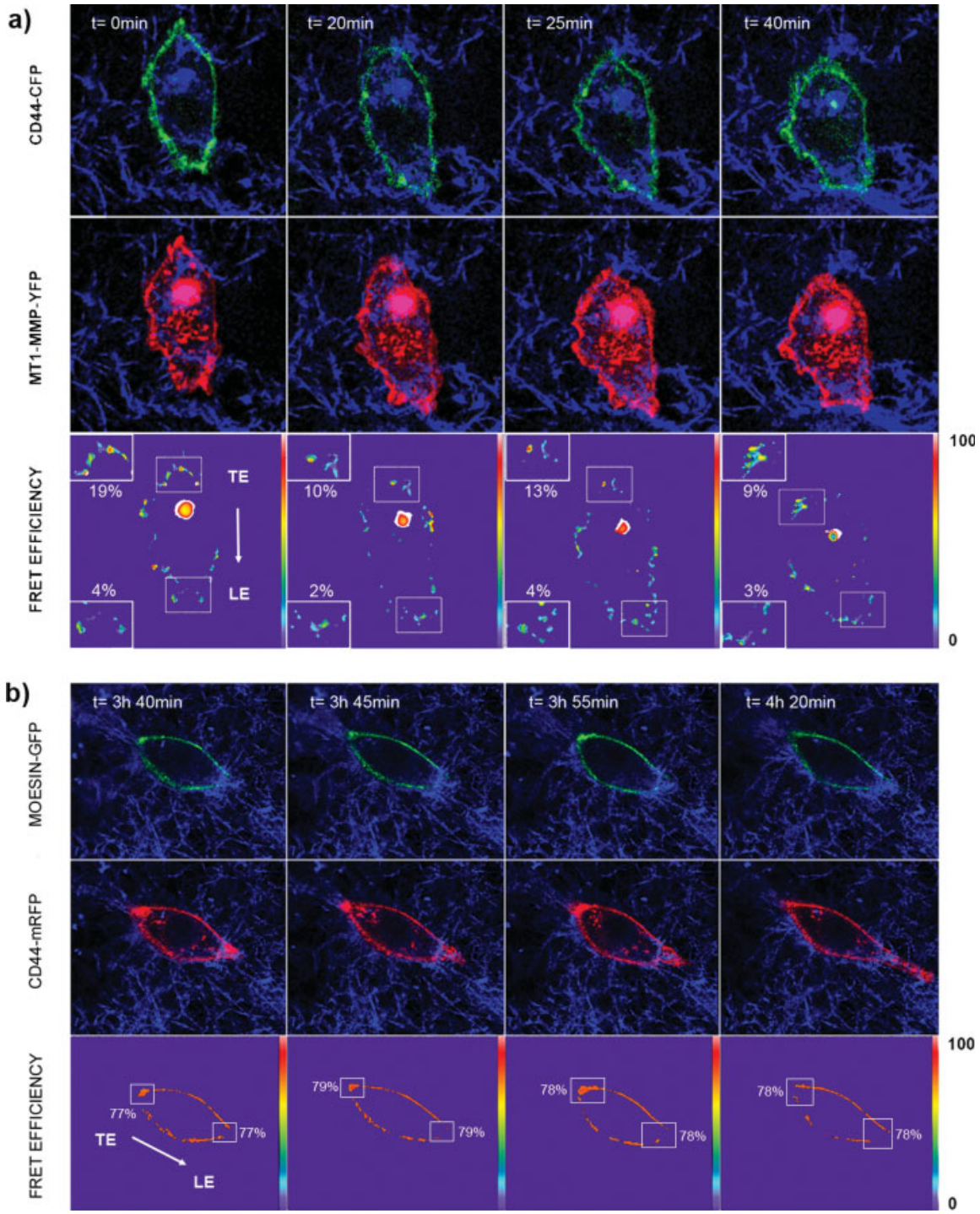

Fig. 3. Dynamic assessment of CD44-MT1-MMP and CD44-moesin interactions in live cell studies of tumor cell invasion. MDA-MB-231 cells were cotransfected with (**a**) CD44-CFP and MT1-MMP-YFP or (**b**) CD44-mRFP and moesin-GFP, and embedded in HA-3D Col I matrices. Representative CFP or GFP (green) and YFP or mRFP (red) fluorescence images superimposed on a reflection image showing collagen fibers (blue) obtained at the times indicated are shown. The arrow indicates the direction of movement. Pseudo-colored λFRET efficiency images include details of the trailing and leading edges (TE and LE) in the upper and lower insets, respectively. The FRET efficiency values calculated in these areas are indicated.

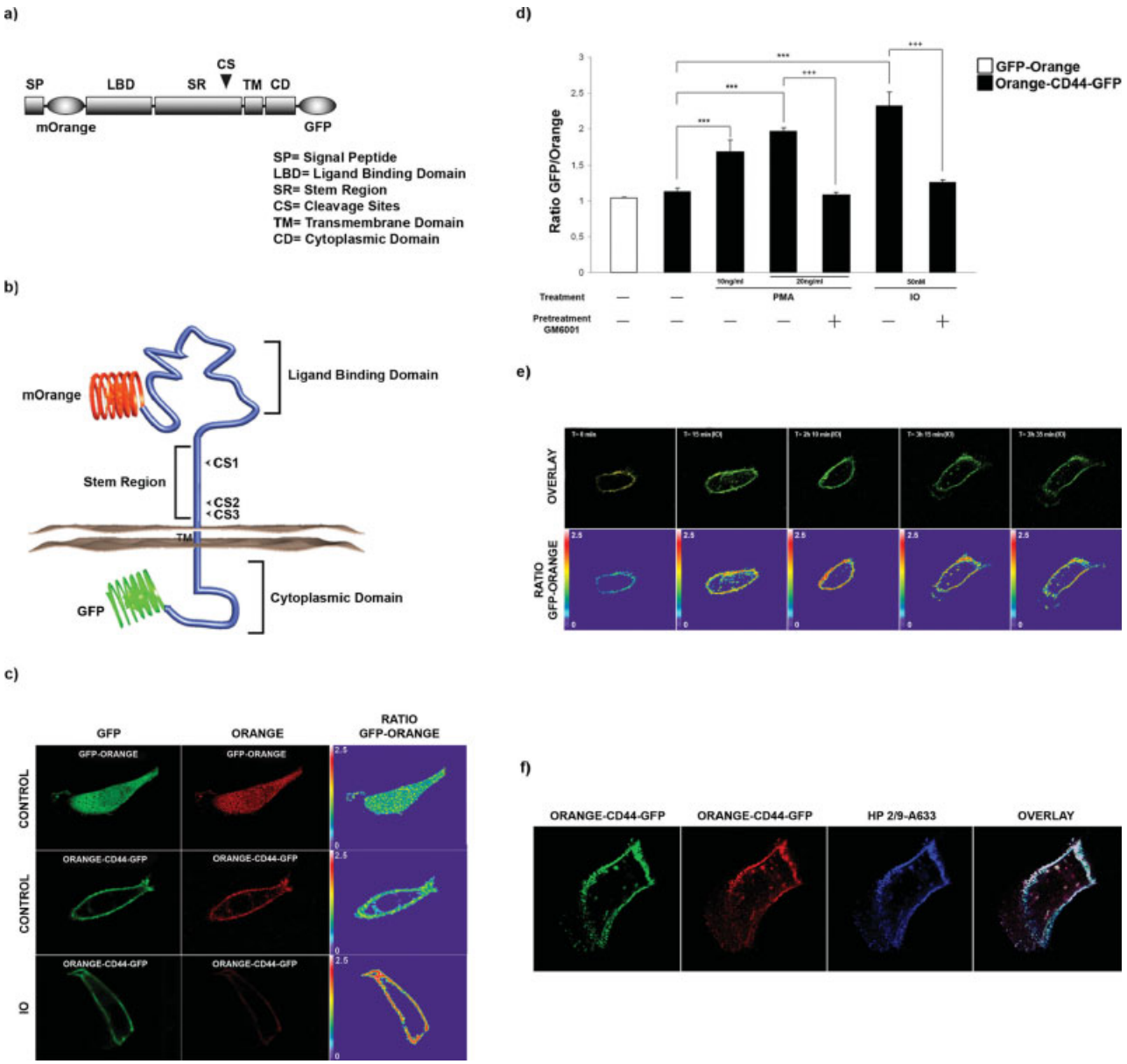

Fig. 4. Design and evaluation of the Orange-CD44-GFP shedding reporter. Schematic representation of the coding sequence (**a**) and structure (**b**) of the Orange-CD44-GFP shedding reporter. (**c**–**f**) MDA-MB-231 cells expressing tandem GFP-Orange or Orange-CD44-GFP were either (c, e) treated with or without IO (50 nM) for 2 h, or (d) pretreated with or without the MMP inhibitor GM6001 (10 μM) for 24 h and incubated with PMA (10 and 20 ng/mL) or IO (50 nM) for an additional 2 h. The cells were either fixed and analyzed by confocal microscopy imaging (c,d) or analyzed by live confocal microscopy imaging (e). (c) Representative GFP and Orange fluorescence images and the resulting GFP/Orange ratio image obtained under confocal microscopy are shown. (d) Bars represent quantification of the GFP/Orange ratio from microscopic images corresponding to 25 cells in three independent experiments. (e) Representative GFP and Orange fluorescence superimposed images and GFP/Orange ratio pseudo-colored images were obtained at the times indicated. (f) MDA-MB-231 cells expressing Orange-CD44-GFP were fixed and stained with anti-CD44 (HP2/9) primary monoclonal antibody and Alexa-633-conjugated anti-mouse secondary antibody. Fluorescence images show Orange (red), GFP (green), or Alexa 633 (blue) fluorescence and their superimposition.

confocal microscope from cells expressing the Orange-CD44-GFP or GFP-Orange construct were used to produce a GFP-Orange ratio image (Fig. 4c). This image represents the relationship between the intracellular and extracellular domains of CD44 within the cell, and is used to quantitatively estimate CD44 cleavage (such as that produced by ionomycin (IO) treatment [Okamoto et al., 1999a]) with sub-cellular resolution (Fig. 4c). The

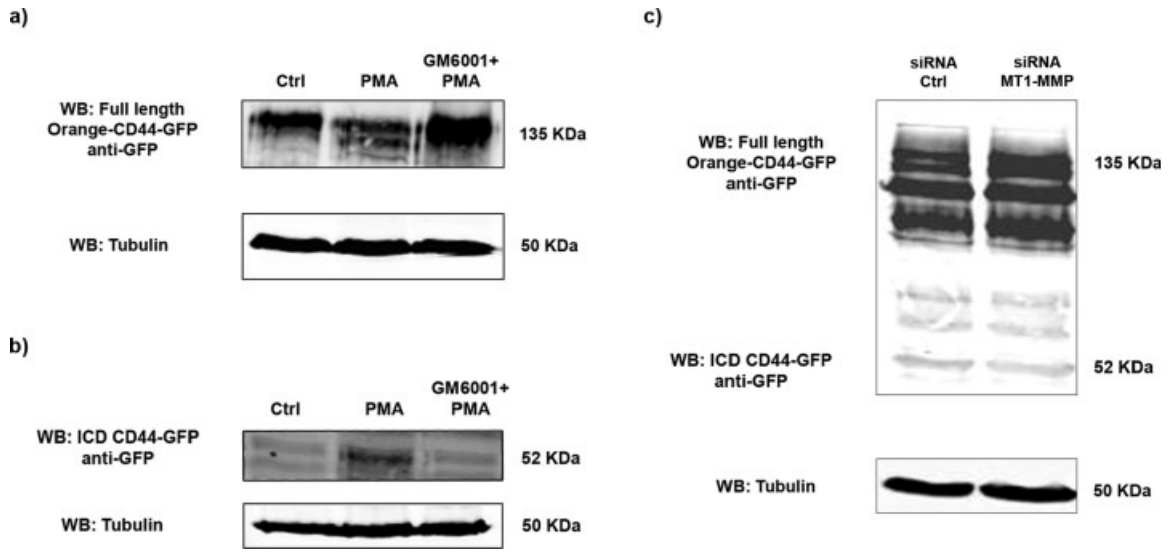

Fig. 5. Biochemical characterization of the Orange-CD44-GFP shedding reporter. (**a**, **b**) HT-1080 cells stably expressing Orange-CD44-GFP were pretreated or not with GM6001 (10 μM) for 24 h and then incubated with PMA (20 ng/mL) for additional 2h. (**c**) MDA-MB-231 cells were transfected with control or MT1-MMP siRNA and Orange-CD44-GFP. Forty-eight hours after, cell lysates were isolated and analyzed by western blotting using polyclonal anti-GFP, or anti-tubulin primary antibody, and Alexa-Fluor-680-conjugated secondary antibodies.

GFP-Orange relationship estimated from the microscopic fluorescence ratio image was quantitatively determined as described in the Materials and Methods section. Analysis of cells treated with the stimulating agents phorbol myristate acetate (PMA) and IO, which have been shown to induce CD44-cleavage, [Okamoto et al., 1999a] in the presence or absence of the MMP inhibitor GM6001, demonstrated that the reporter was subject to proteolytic processing (Fig. 4d). Monitoring the kinetics of IO induced CD44 cleavage further validated its use as a shedding reporter in live cell microscopy studies (Fig. 4e). We further tested this construct by immunolocalizing the Orange (red) and GFP (green) signals with anti-CD44 antibody staining (blue), which confirmed the overlap of the fluorescence signals and that the CD44 membrane localization pattern was not altered (Fig. 4f). Colocalization analysis is shown (Supporting Fig. 2). Moreover, expression of the Orange-CD44-GFP reporter induced an increase of 39.6% in cell invasion which was inhibited by GM6001 protease inhibitor (Supporting Fig. 3), thus revealing it retains some functional properties of the CD44 molecule. Biochemical studies were carried out to further evaluate the CD44 shedding reporter. PMA treatment induced a reduction in the 135 kD band corresponding to full length Orange-CD44-GFP reporter (Fig. 5a). The 52 kD intracellular CD44-GFP domain was detected in the cell lysates (Fig. 5b). Cleavage was inhibited by pretreating the cells with the MMP inhibitor GM6001 (Figs. 5a and 5b), or by transfecting cells with MT1-MMP siRNA (Fig. 5c) which induced an increased 135 kD full length Orange-CD44-GFP band and the reduction of 52 kD intracellular CD44-GFP band.

MDA-MB-231 cells expressing the shedding reporter were plated on coverslips coated or not with HA, or HA-3D Col I matrices, to determine the effect of the extracellular microenvironment on CD44 cleavage ''in vivo''. These studies showed that HA-3D Col I induced CD44 release globally at the cell surface, which was greater than that induced on HA-coated surfaces. Importantly, the shedding of the Orange-CD44-GFP reporter expressed in cells plated on HA-3D Col I was completely abolished by function-blocking antibodies directed against MT1-MMP [Galvez et al., 2002] (Figs. 6a and 6c). To further clarify this point we analyzed cells transfected with MT1-MMP siRNA, which showed impaired CD44 cleavage in HA-Col I surfaces (Figs. 6b and 6d). Together, these results demonstrate that MT1-MMP is responsible for CD44 cleavage in our invasion model. We then monitored the dynamics of CD44 release and its localization in different plasma membrane sub-domains by analyzing the sequences of the GFP/Orange ratio images of live cells invading HA-3D Col I (Figs. 7a and 7b). This analysis revealed that CD44 shedding occurs preferentially at the retracting trailing edge during cell migration. These results support a role for the CD44-MT1-MMP interaction and subsequent CD44 processing in cell trailing-edge detachment, possibly by the MT1-MMP-mediated release of CD44-dependent

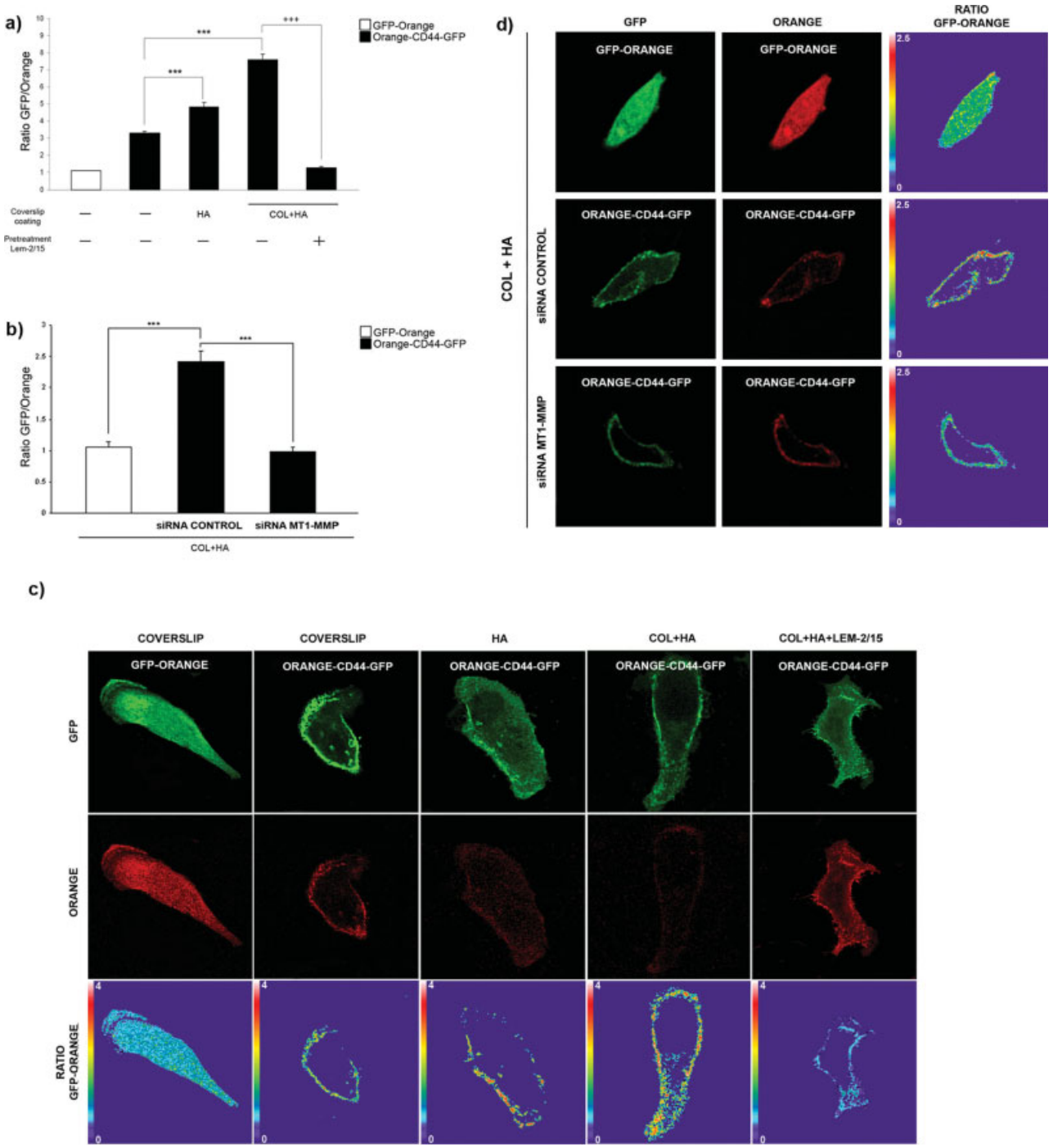

Fig. 6. MT1-MMP-dependent proteolytic processing of CD44 extracellular domain is induced in 3D HA-Col I matrices. MDA-MB-231 cells were transfected with the tandem GFP-Orange or Orange-CD44-GFP constructs. (**a**, **c**) Cells incubated with or without function-blocking anti-MT1-MMP (Lem-2/15) monoclonal antibody (10 μg/mL) were plated on coverslips coated or not with HA-3D Col I or HA, and were then fixed and analyzed by confocal microscopy imaging. (**b**, **d**) Cells were transfected with a control or MT1-MMP specific siRNA and plated on HA-3D Col I coated coverslips (a, b) The GFP/Orange ratio was quantified from 25 cells in three independent experiments and is represented in the bar diagrams. (c,d) Images show GFP and Orange fluorescence (green and red, respectively) and the GFP/Orange ratio (pseudo-colored).

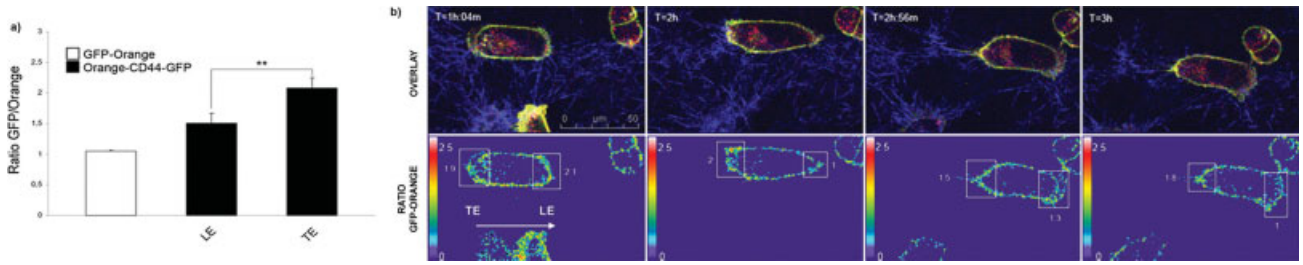

Fig. 7. Proteolytic cleavage of CD44 by MT1-MMP occurs preferentially at the trailing edge during tumor cell invasion. Cells expressing Orange-CD44-GFP were embedded in 3D HA-Col I matrices and analyzed by live confocal imaging. (**a**) Bars represent the GFP/Orange ratio values calculated at leading (LE) or trailing edges (TE) from 25 cells in three independent experiments. (**b**) Representative GFP-Orange fluorescence images superimposed on a reflection image showing collagen fibers (blue) and the GFP/Orange ratio pseudo-colored images were obtained at the times indicated. The GFP/Orange ratio pseudo-colored images include details of the trailing and leading edges, and the GFP/Orange ratio values calculated in these areas are indicated. The arrow indicates the direction of movement.

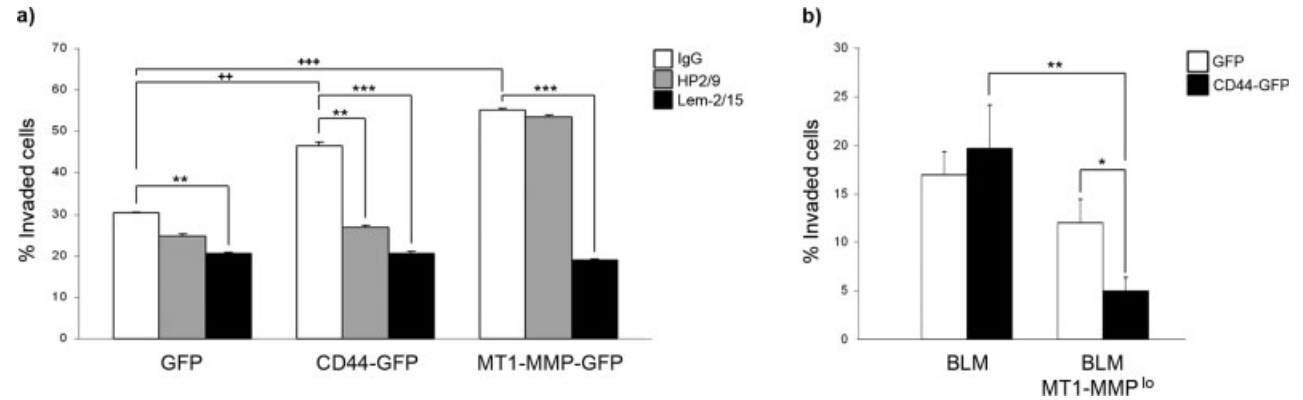

Fig. 8. CD44- and MT1-MMP-dependence of tumor cell invasion of HA-3D Col matrices. MDA-MB-231 (**a**) or BLM (**b**) cells were transfected with GFP, CD44-GFP, or MT1-MMP-GFP and then allowed to migrate for 48 h on transwell filters coated with 3D HA-Col I to 10% fetal bovine serum (FBS)-containing medium in the presence of isotype control IgG, function-blocking anti-CD44 antibody (HP2/9), or anti-MT1-MMP (Lem-2/15) antibody (10 μg/mL). Bars represent the percentages of invading GFP-expressing cells quantified in four different fields for each of the seven independent experiments performed.

cell-matrix bonds, which would in turn promote cell movement.

MT1-MMP-Dependence of CD44-Mediated Tumor Cell Invasion on Collagen Matrices

Our previous results allowed us to hypothesize that MT1-MMP is required for CD44-mediated invasion by promoting the proteolytic cleavage of CD44 at the trailing edge of the cell during retraction. The interdependence of CD44 and MT1-MMP in their invasion-promoting activities was investigated by performing transwell invasion assays of MDA-MB-231 cells over-expressing CD44 and MT1-MMP in the presence or absence of function-blocking antibodies directed against these molecules. Our results show that CD44 over-expression induced a significant increase in invasion and function blocking antibodies against CD44 [Lara-Pezzi et al., 2001] inhibited this effect (Fig. 8a). Blocking MT1-MMP function diminished both MT1-MMP- and CD44-mediated invasion, whereas blocking CD44 function did not affect the invasion induced by MT1-MMP (Fig. 8a). These results indicate that CD44-dependent invasion requires MT1-MMP functionality, whereas CD44 is not essential for MT1-MMP-mediated invasion. Melanoma BLM cells presented a decreased invasive capacity when the MT1-MMP gene was silenced (MT1-MMP^{lo}). It is important to note that the expression of CD44-GFP induced a 16% increase in cell invasion compared with that induced by GFP in cells with intact MT1-MMP activity. On the contrary, in the absence of this protease, MT1-MMP^{lo} BLM cells, CD44-GFP expression produced a 74% inhibition of cell invasion compared to control GFP expressing (Fig. 8b). In summary, an excess of CD44 surface molecules promoted invasion under physiological conditions, whereas it impaired the invasive capacity of cells in which MT1-MMP had been inacti-

vated. Thus, CD44 involvement in cell invasion depends on its levels of expression at the cell surface and the activity of MT1-MMP in our invasion model.

DISCUSSION

This study addresses, for the first time, the in vivo CD44-MT1-MMP interaction and CD44 shedding using live cell confocal microscopy. Three dimensional collagen matrices used in our study mimic the ''in vivo'' environment encountered in tissues surrounding tumours, which are more fibrous than normal tissues because of the increased deposition of fibrillar collagen and HA being associated with higher Col I fibre density and HA expression levels [Toole et al., 1979; Zhang et al., 1995; Wang et al., 2002]. It therefore represents an ideal model in which to study tumour cell invasion in vitro. We used state of the art technology to perform this study; namely the new λFRET method, which has been validated with structurally characterized FRET standards of variable lengths demonstrating its outstanding performance compared with well-established FRET methods in terms of sensitivity [Megías et al., In press]. We used λFRET to study the in vivo interaction of CD44 with its partners because its weakness requires a highly sensitive FRET analysis method, and because it enabled us to monitor FRET in live cells. The FRET efficiency values obtained for CD44-MT1-MMP interaction were low, and were restricted to certain areas of the cell perimeter. Due to these facts, we performed extensive quantifications using two different FRET analysis methods, which showed that, although faint, the results were highly consistent thus demonstrating the physiological relevance of the results presented herein.

The importance of CD44 shedding in the pathogenesis of human tumors has been highlighted by several reports that show in situ the CD44 cleavage product enriched in human tumor tissues compared with that in the surrounding normal tissues [Okamoto et al., 2002; Nakamura et al., 2004]. We developed a technologically innovative tool for the study of CD44 shedding which proved to be very useful for monitoring the sub-cellular localization of the proteolitic processing of CD44, a matter that could not be explored with the techniques available up to date. This technology should prove to be useful in the future for the study of a number of membrane molecules, which are subjected to ecto-domain shedding as a mechanism underlying their functional regulation being key for physiopathologically relevant processes [Nagano and Saya, 2004; Garton et al., 2006].

The CD44-MT1-MMP interaction is here shown to be finely regulated at the cell surface during the invasion process, with preferential localization at the retracting trailing edge, where CD44 proteolytic cleavage was also shown to be enriched. CD44 proteolytic processing in this 3D Col I was shown to be MT1-MMP dependent, since it was abolished by function blocking antibodies and siRNA silencing of this molecule. In our cell invasion model, an increase in the levels of surface CD44 promoted cell invasion when activity of MT1-MMP was intact, whereas it had the opposite effect in the absence of MT1-MMP. These results may be explained by the the fact than an increased expression of CD44 provides new adhesive contacts that firmly attach the cells to the substrate and must be released by the MT1-MMP-mediated cleavage of the extracellular domain to allow cell motility. We propose a role of MT1-MMP-dependent CD44 proteolytic processing in releasing cell contacts to the ECM at the trailing edge of the cell allowing rear detachment required for the forward movement of the cell during invasion. Thus, CD44 can exert a pro-, anti-invasive or have no effect on the invasive ability of tumour cells in a manner, that is, dependent on its levels of expression at the cell surface and the activity of MT1-MMP. This may help to explain contradictory conclusions regarding the correlation between CD44 expression and the migratory and invasive ability of tumour cell lines, the metastatic capacity of cancer cells and cancer disease prognosis [Driessens et al., 1995; Maaser et al., 1999; Naor et al., 2002; Weber et al., 2002].

It has been shown that CD44 is responsible for MT1-MMP delivery to the leading edges of migrating cells [Mori et al., 2002]. This does not seem to be the case in our invasion model, because a blocking anti-CD44 antibody did not affect MT1-MMP-mediated invasiveness. However, we cannot rule out this possibility because the MT1-MMP-CD44 interaction was also detected at the leading edge in our studies The localization of CD44 and MT1-MMP molecules at the lamellipodia of migrating cells [Kajita et al., 2001; Mori et al., 2002] supports the prevailing hypothesis that proposes a role for CD44 as a platform for the presentation of MT1-MMP and other MMPs, such as MMP9 at the leading edge of the cell [Itoh and Seiki, 2006]. These studies addressed the protein domains involved in CD44-MT1-MMP interaction and developed deletion mutants to abolish the interaction, which inhibited CD44 shedding and perturbed cell migration [Kajita et al., 2001; Mori et al., 2002]. The data presented herein reveal novel functional implications of CD44-MT1-MMP interplay that are in accordance with the afore mentioned works. The extracellular context composition, probably the presence of fibrillar collagen, which was shown to promote CD44 shedding, is most likely responsible for the novel MT1-MMP-dependent regulation of CD44-mediated invasion described herein. Accordingly, previous studies have demonstrated the differential regulation of MT1-MMP depending on the composition of the extra-

cellular matrix, showing that Col I promotes MT1 activation, redistribution to specialized membrane microdomains and specific sub-cellular localization [Galvez et al., 2002; Annabi et al., 2004]. Moreover, our previous studies showed that MT1-MMP is relocalized to a different intracellular vesicle trafficking compartment when cells are embedded in 3D Col I matrices [Bravo-Cordero et al., 2007]. This study uncovered a Rab8-mediated exocytic traffic capable of delivering MT1-MMP to invasive structures which may represent a physiologically relevant pathway of MT1-MMP regulation during tumour cell invasion of collagen rich tissues, such as those surrounding tumours.

MT1-MMP is one of the most critical factors in the invasive machinery of tumor cells because its overexpression enhances the invasive capacity of cells and its silencing suppresses cell migration and invasion [Egeblad and Werb, 2002]. MT1-MMP pro-invasive activity is based on its ability to degrade ECM proteins and activate soluble MMPs, like pro-MMP2, and processing cytokines and surface receptors, including integrins and the CD44 adhesion molecule [Sato et al., 2005]. These processes have been ascribed to the leading edge of the cell. Moreover, our studies reveal a novel aspect of MT1-MMP pro-invasive activity by highlighting its role at the retracting cell rear during the invasion process. Our study provides a novel perspective for MT1-MMP-dependent functional regulation of CD44 which should prove to be very useful considering the importance of MT1-MMP in tumour cell invasion and angiogenesis, which makes this enzyme a key molecular target for cancer therapeutics.

ACKNOWLEDGMENTS

The authors thank Dr. A.G. Arroyo for critical reading of the manuscript, Drs. Mizoi, Sánchez-Madrid, del Pozo, and Tsien are acknowledged for providing us with reagents.

REFERENCES

Annabi B, Thibeault S, Moumdjian R, Beliveau R. 2004. Hyaluronan cell surface binding is induced by type I collagen and regulated by caveolae in glioma cells. J Biol Chem 279(21):21888–21896.

Bartolome RA, Molina-Ortiz I, Samaniego R, Sanchez-Mateos P, Bustelo XR, Teixido J. 2006. Activation of Vav/Rho GTPase signaling by CXCL12 controls membrane-type matrix metalloproteinase-dependent melanoma cell invasion. Cancer Res 66(1):248–258.

Bravo-Cordero JJ, Marrero-Diaz R, Megías D, Genís L, García-Grande A, García MA, Arroyo AG, Montoya MC. 2007. MT1-MMP pro-invasive activity is regulated by a novel Rab8-dependent exocytic pathway. EMBO J 26(6):1499–1510.

Driessens MH, Stroeken PJ, Rodriguez Erena NF, van der Valk MA, van Rijthoven EA, Roos E. 1995. Targeted disruption of CD44 in MDAY-D2 lymphosarcoma cells has no effect on subcutaneous growth or metastatic capacity. J Cell Biol 131(6 Part 2):1849–1855.

Egeblad M, Werb Z. 2002. New functions for the matrix metalloproteinases in cancer progression. Nat Rev Cancer 2(3):161–174.

Friedl P, Maaser K, Klein CE, Niggemann B, Krohne G, Zanker KS. 1997. Migration of highly aggressive MV3 melanoma cells in 3-dimensional collagen lattices results in local matrix reorganization and shedding of alpha2 and beta1 integrins and CD44. Cancer Res 57(10):2061–2070.

Friedl P, Wolf K. 2003. Tumour-cell invasion and migration: Diversity and escape mechanisms. Nat Rev Cancer 3(5):362–374.

Galvez BG, Matias-Roman S, Yanez-Mo M, Sanchez-Madrid F, Arroyo AG. 2002. ECM regulates MT1-MMP localization with beta1 or alphavbeta3 integrins at distinct cell compartments modulating its internalization and activity on human endothelial cells. J Cell Biol 159(3):509–521.

Garton KJ, Gough PJ, Raines EW. 2006. Emerging roles for ectodomain shedding in the regulation of inflammatory responses. J Leukoc Biol 79(6):1105–1116.

Itoh Y, Seiki M. 2006. MT1-MMP: A potent modifier of pericellular microenvironment. J Cell Physiol 206(1):1–8.

Kajita M, Itoh Y, Chiba T, Mori H, Okada A, Kinoh H, Seiki M. 2001. Membrane-type 1 matrix metalloproteinase cleaves CD44 and promotes cell migration. J Cell Biol 153(5):893–904.

Lara-Pezzi E, Serrador JM, Montoya MC, Zamora D, Yanez-Mo M, Carretero M, Furthmayr H, Sanchez-Madrid F, Lopez-Cabrera M. 2001. The hepatitis B virus X protein (HBx) induces a migratory phenotype in a CD44-dependent manner: Possible role of HBx in invasion and metastasis. Hepatology 33(5):1270–1281.

Legg JW, Lewis CA, Parsons M, Ng T, Isacke CM. 2002. A novel PKC-regulated mechanism controls CD44 ezrin association and directional cell motility. Nat Cell Biol 4(6):399–407.

Lehti K, Valtanen H, Wickstrom SA, Lohi J, Keski-Oja J. 2000. Regulation of membrane-type-1 matrix metalloproteinase activity by its cytoplasmic domain. J Biol Chem 275(20):15006–15013.

Maaser K, Wolf K, Klein CE, Niggemann B, Zanker KS, Brocker EB, Friedl P. 1999. Functional hierarchy of simultaneously expressed adhesion receptors: Integrin alpha2beta1 but not CD44 mediates MV3 melanoma cell migration and matrix reorganization within three-dimensional hyaluronan-containing collagen matrices. Mol Biol Cell 10(10):3067–3079.

Marhaba R, Zoller M. 2004. CD44 in cancer progression: Adhesion, migration and growth regulation. J Mol Histol 35(3):211–231.

Megías D, Marrero-Diaz R, Martínez del Peso B, Bravo-Cordero JJ, García MA, Santos A, Montoya MC. In press. Novel lambda FRET spectral confocal microscopy imaging method. Microsc Res Tech 10: in press..

Mori H, Tomari T, Koshikawa N, Kajita M, Itoh Y, Sato H, Tojo H, Yana I, Seiki M. 2002. CD44 directs membrane-type 1 matrix metalloproteinase to lamellipodia by associating with its hemopexin-like domain. EMBO J 21(15):3949–3959.

Nagano O, Saya H. 2004. Mechanism and biological significance of CD44 cleavage. Cancer Sci 95(12):930–935.

Nakahara H, Howard L, Thompson EW, Sato H, Seiki M, Yeh Y, Chen WT. 1997. Transmembrane/cytoplasmic domain-mediated membrane type 1-matrix metalloprotease docking to invadopodia is required for cell invasion. Proc Natl Acad Sci USA 94(15):7959–7964.

Nakamura H, Suenaga N, Taniwaki K, Matsuki H, Yonezawa K, Fujii M, Okada Y, Seiki M. 2004. Constitutive and induced CD44

shedding by ADAM-like proteases and membrane-type 1 matrix metalloproteinase. Cancer Res 64(3):876–882.

Naor D, Nedvetzki S, Golan I, Melnik L, Faitelson Y. 2002. CD44 in cancer. Crit Rev Clin Lab Sci 39(6):527–579.

Okamoto I, Kawano Y, Matsumoto M, Suga M, Kaibuchi K, Ando M, Saya H. 1999a. Regulated CD44 cleavage under the control of protein kinase C, calcium influx, and the Rho family of small G proteins. J Biol Chem 274(36):25525–25534.

Okamoto I, Kawano Y, Tsuiki H, Sasaki J, Nakao M, Matsumoto M, Suga M, Ando M, Nakajima M, Saya H. 1999b. CD44 cleavage induced by a membrane-associated metalloprotease plays a critical role in tumor cell migration. Oncogene 18(7):1435–1446.

Okamoto I, Tsuiki H, Kenyon LC, Godwin AK, Emlet DR, Holgado-Madruga M, Lanham IS, Joynes CJ, Vo KT, Guha A, Matsumoto M, Ushio Y, Saya H, Wong AJ. 2002. Proteolytic cleavage of the CD44 adhesion molecule in multiple human tumors. Am J Pathol 160(2):441–447.

Sato H, Takino T, Miyamori H. 2005. Roles of membrane-type matrix metalloproteinase-1 in tumor invasion and metastasis. Cancer Sci 96(4):212–217.

Suenaga N, Mori H, Itoh Y, Seiki M. 2005. CD44 binding through the hemopexin-like domain is critical for its shedding by membrane-type 1 matrix metalloproteinase. Oncogene 24(5):859–868.

Taraboletti G, D'Ascenzo S, Borsotti P, Giavazzi R, Pavan A, Dolo V. 2002. Shedding of the matrix metalloproteinases MMP-2, MMP-9, and MT1-MMP as membrane vesicle-associated components by endothelial cells. Am J Pathol 160(2):673–680.

Toole BP, Biswas C, Gross J. 1979. Hyaluronate and invasiveness of the rabbit V2 carcinoma. Proc Natl Acad Sci USA 76(12):6299–6303.

Tsukita S, Oishi K, Sato N, Sagara J, Kawai A. 1994. ERM family members as molecular linkers between the cell surface glycoprotein CD44 and actin-based cytoskeletons. J Cell Biol 126(2):391–401.

Vivinus-Nebot M, Rousselle P, Breittmayer JP, Cenciarini C, Berrih-Aknin S, Spong S, Nokelainen P, Cottrez F, Marinkovich MP, Bernard A. 2004. Mature human thymocytes migrate on laminin-5 with activation of metalloproteinase-14 and cleavage of CD44. J Immunol 172(3):1397–1406.

Wang W, Wyckoff JB, Frohlich VC, Oleynikov Y, Huttelmaier S, Zavadil J, Cermak L, Bottinger EP, Singer RH, White JG, Segall JE, Condeelis JS. 2002. Single cell behavior in metastatic primary mammary tumors correlated with gene expression patterns revealed by molecular profiling. Cancer Res 62(21):6278–6288.

Weber GF, Bronson RT, Ilagan J, Cantor H, Schmits R, Mak TW. 2002. Absence of the CD44 gene prevents sarcoma metastasis. Cancer Res 62(8):2281–2286.

Wolf K, Wu YI, Liu Y, Geiger J, Tam E, Overall C, Stack MS, Friedl P. 2007. Multi-step pericellular proteolysis controls the transition from individual to collective cancer cell invasion. Nat Cell Biol 9(8):893–904.

Zhang L, Underhill CB, Chen L. 1995. Hyaluronan on the surface of tumor cells is correlated with metastatic behavior. Cancer Res 55(2):428–433.